Available online at www.CivileJournal.org

Civil Engineering Journal

(E-ISSN: 2476-3055; ISSN: 2676-6957)

Vol. 10, No. 07, July, 2024

Evaluating the Efficiency of Alkaline Activator with Silica-Rich Wastes in Stabilizing Cadmium-Contaminated Soil

Khitam Saeed [1], Sahar Al-Khyat [1], Zuhair Abd Hacheem [1], Sabah H. Fartosy [1*]

[1] *Department of Water Resources Engineering, College of Engineering, Mustansiriyah University, Baghdad, 10047, Iraq.*

Received 05 March 2024; Revised 28 May 2024; Accepted 09 June 2024; Published 01 July 2024

Abstract

Contaminant soil remediation has potential engineering applications with various stabilization techniques addressing heavy metal contamination. Conventional soil stabilizers, however, have an environmental impact, promoting international research into environmentally friendly alternatives. Using waste byproducts to produce geopolymer binders as new green cementitious materials can provide an environmentally friendly and effective option for soil improvement. Silica-rich wastes have been advanced as a sustainable option for soil stabilization. The effectiveness of alkaline-activated silica-rich wastes in stabilizing cadmium-contaminated soil and its potential engineering utilization remain of profound significance, demanding sustained and rigorous research investigation. Cadmium was immobilized in silty clay soil by rich silica waste products—fly ash, silica fume, and rice husk ash—at various percentages with 4.5 and 6.5-molar alkaline activators. Unconfined compressive strength tests assessed soil behavior, while Toxicity Characteristic Leaching Procedure (TCLP), pH tests, X-ray diffraction, and scanning electron microscope analyses explained cadmium immobilization mechanisms. The experimental results revealed that alkali-activated silica-rich wastes enhanced strength and cementitious properties and reduced cadmium leaching in the contaminated silty clay. The Finite Element Method was also employed to analyze the bearing capacity of the stabilized contaminated soil. The numerical results support the experimental results and confirm increased soil strength and reduced compressibility, endorsing the efficacy of the stabilization techniques and environmental benefits.

Keywords: Soil Stabilization; Fly Ash; Rice Husk Ash; Silica Fume; Product Waste Materials, Bearing Capacity, Settlement.

1. Introduction

The inevitable expansion of soil contamination can be attributed to several interconnected factors stemming from industrialization. Cadmium (Cd), a contaminant, accumulates in soils and is commonly produced from geological, anthropogenic, and human activities [1]. It is a highly toxic heavy metal that poses serious dangers to human health and the environment, even at low doses [2]. Remediation of cadmium-contaminated soil has become increasingly crucial since cadmium has detrimental impacts on human health and the environment. Conventional techniques for remediating soil, including lime and cement, have been frequently found to be expensive, intrusive, and harmful to the ecosystem. Thus, there is an urgent need for creative, long-lasting, and economical methods of reducing cadmium pollution.

Recent remediation techniques that are effectively used for metals-contaminated soils are biological, agricultural technology, and physicochemical methods [3–5]. The physicochemical method, which includes extraction, stabilization, and solidification, is used in the current study. Heavy metal-polluted soils can now be correctly and economically dealt with using derivative waste. The physicochemical process of solidification/stabilization (S/S) gives vast remediation for polluted soil by considerably lowering the potential and solubility of heavy metals in sediments [3, 5].

* Corresponding author: dr.sabah77@uomustansiriyah.edu.iq

http://dx.doi.org/10.28991/CEJ-2024-010-07-04

Silica-rich wastes, such as fly ash, silica fume, and rice husk ash, have been widely used to stabilize contaminated soil. Khan et al. [6] investigated the results of changing cement with rice husk ash (RHA) at the compressive energy and leachability of stabilized sediments heavy metals. The more potent the solidified sample's power, the decrease the quantity of cadmium leaching within the Toxicity Characteristic Leaching Procedure (TCLP). The reports of X-ray diffraction confirmed that $Cd(NO_3)_2$ produced CdOH forms. The research by Charyulu et al. [7] attempted to improve the stability of unsuitable soil for construction by combining rice husk ash with cement. The soil mixed with various percentages of RHA (5%, 10%, and 15%) at a consistent amount of cement showed promising results in enhancing stability and improving properties. Several researchers have studied the stabilization effect of silica fume (SF) on contaminated soil [8–10]. These studies showed that SF could enhance polluted soils' chemical, mechanical, and physical characteristics by increasing their liquid and plastic limits and optimal water content while decreasing the maximum dry densities and improving the shear strength characteristics.

Alkali activation forms geopolymers in amorphous silica-rich materials by starting the pozzolanic reaction using alkaline solutions [11]. These geopolymers are good candidates for soil remediation applications due to their superior binding qualities and chemical stability. Certain experimental studies used silica-rich wastes to solidify the soil contaminated by the geopolymer mechanism. Chemically treated cadmium-polluted soil with 450 ppm using alkali-activated materials with rich silica materials, including fly ash, silica fumes, and rice husk ash, at a dose of 20 percent was investigated by Muhammad et al. [12]. The strength results revealed that the unconfined compressive strength (UCS) values were above the prescribed value of 0.35 MPa of the U.S. EPA. The TCLP findings showed that the Cd collected from soils mixed with 20% cemented materials after 14 days and 28 days was close to 0.25 mg/L, far below the 5 mg/L (TCLP regulatory limit). The XRD results also indicated that cadmium immobilization was due to C-S-H formation [12]. The effectiveness of alkaline activation of low-calcium fly ash on the enhancement of residual granite soils was approved by Cristelo et al. [13]. The findings demonstrated that the Si: Al and Na: Si ratios are completely related to strength development.

In Cd-contaminated soil, Wang et al. [14] examined the stabilizing effects of alkali-activated fly ash and Ground Granulated Blast Slags (GGBS) geopolymer. It found that Cd leaching decreased as the curing duration and geopolymer content increased. Rios et al. [15] Performed experiments on silty soil stabilized with geopolymers from low-calcium fly ash and an alkaline made from sodium hydroxide and sodium silicate. With this treatment, unconfined compression resistance and seismic wave testing at different mixes significantly increased strength and stiffness. A study using experiments was conducted to evaluate the development of the resistance of clay soil using an activated alkali of 1 molar sodium silicate with a NaOH concentration of 8, 10, and 12 molars and mixed in a 2:1 ratio. Fly ash remained at 10, 15, and 20% [16–18]. The results presented successive progress in the soil strength. Turan et al. [19] The study investigates using alkali-activated fly ash to improve clay soil, demonstrating enhanced compressive strength. The greatest compressive strength of 1293 kPa was achieved at alkali doses of 12% to 16% with a silica modulus of 1.25. Researchers looked at using bischofite and an alkaline activator to enhance laterite soils strength and microstructural features [20], showing the highest uniaxial compressive strength (UCS) at an optimal mix design and indicating improved soil bonding between magnesium, silica, and alumina compounds.

It can be noted that most studies on metal solidification/stabilization in soil/sediments have focused on either using traditional stabilizers alone or in combination with other pozzolans. Limited research has been done on solidifying heavy metal contaminated soil using pozzolan materials with alkaline activators and exploring the potential utilization of the stabilized Cd soils for engineering projects. Therefore, the main objective of this study is to examine the stabilizing effect of an alkaline activator with silica-rich wastes on soil contaminated with cadmium, investigate the mechanisms that underlie this process, and numerically evaluate its potential for engineering purposes. This study aims to provide new perspectives on a sustainable method of remediating contaminated soil by utilizing alkali-activated materials on cadmium-contaminated soil.

2. Material and Methods

2.1. Experimental Program

The soil employed in this study was taken at a depth of one meter from the Al-Tamyra region, which lies north of Baghdad [21]. Following the ASTM standards, several geotechnical tests were conducted on the soil. Based on the percentages of soil particle size and plasticity properties, the soil was classified as Silty Clay Loam according to the USDA or Lean Clay (CL) according to USCS. The physical, chemical, and compaction properties of the soil are given in Table 1.

Table 1. Physical, chemical, and compaction properties of the soil

Physical Properties	Value
Particle size distribution	
Sand (%)	13
Silt (%)	57
Clay (%)	30
Liquid Limit (%)	39
Plastic Limit (%)	25
Plasticity Index (%)	14
Maximum dry density (gm/cc)	1.89
Optimum moisture content (%)	18
Natural water content (%)	5
Specific gravity	2.48
PH	7.51
EC	(2.225) (mS/cm)
Soil classification USDA	Silty Clay Loam
Soil classification USCS	CL-Lean Clay

The silty clay soil was contaminated with cadmium by adding 1500 ppm of Cd $(NO_3)^2$. Three waste materials, fly ash, silica fume, and rice husk, stabilized the cadmium-contaminated soil. The fly ash was categorized as Class F with less than 10% calcium oxide and was originally obtained from thermoelectric coal-fired at the Portuguese power plant. The silica fume used was gray, with a relative density of 2.25. Both the fly ash and silica fume were commercially available materials. The rice husk was obtained from rice farms in southern Iraq. It was burned in the furnace for 6 hours at 700 °C controlled temperature with a heating rate of 5 °C/min. Burning rice husks at 700°C creates rice husk ashes with significant pozzolanic activity. The rice husk ashes were then processed using a mechanical grinder to produce ash that passed through a filter with a size opening of 75μm [22]. The chemical components of these materials are summarized in Table 2. The materials used as alkaline activators were sodium silicate (Na_2SiO_3) and sodium hydroxide (NaOH). The sodium silicate solution had a specific gravity of 1.54 g/cm3 and was composed of 13.4% sodium oxide (Na_2O) with 32.5% SiO_2. With a specific gravity of 2.11, a molecular weight of 40 g/mol, and a purity of 95%–99%, the sodium hydroxide was of a flocculent type.

Table 2. Chemical Composition of Soil and by-product waste materials detected by X-ray Fluorescence XRF [22]

	CaO	Al_2O_3	SiO_2	MgO	Fe_2O_3	K_2O	P_2O_5	Other Elements
Soil (%)	22.04	11.44	45.42	5.83	9.76	1.274	0.90	3.34
Fly Ash (FA)	2.41	0.39	86.68	1.41	3.63	2.81	0.76	0.66
Silica Fume (SF)	1.42	0.45	96.45	0.003	0.11	0.44	0.72	1.13
Rice Husk Ash (RHA)	2.87	0.05	88.19	0.84	0.33	4.25	1.28	2.19

All collected soil samples were air-dried to prepare the contaminated soil to keep its compaction and plasticity properties [23]. The samples were then pulverized using a mechanical blender, passed through a 2 mm sieve as recommended by the ASTM standard, and stored in clean plastic bags. To obtain an artificially contaminated soil with metallic cadmium, the doped soil was produced by mixing a specific quantity of cadmium (produced by British Drug House, England's BDH) to reach 1500 mg/kg in polluted concentration. This concentration was prepared by adding 60 g of cadmium to 4.25 liters of distilled water, sufficient to add 25 kg of soil with a required optimum % water content of 18%. The prepared solution was sprayed on the soil and mixed thoroughly. The Cd-doped soil was then stored in a closed bucket and allowed to cure for seven days.

To prepare stabilized contaminated soil, representative amounts of silica-rich materials must be added to replicate the field condition. The three rich-silicon materials, fly ash (FA), rice husk ash (RHA), and silica fume (SF), were mixed with the prepared contaminated soil at three percentages of 10%, 15%, and 20% as substitute content (soil: ash). The research methodology steps are presented in the flowchart in Figure 1.

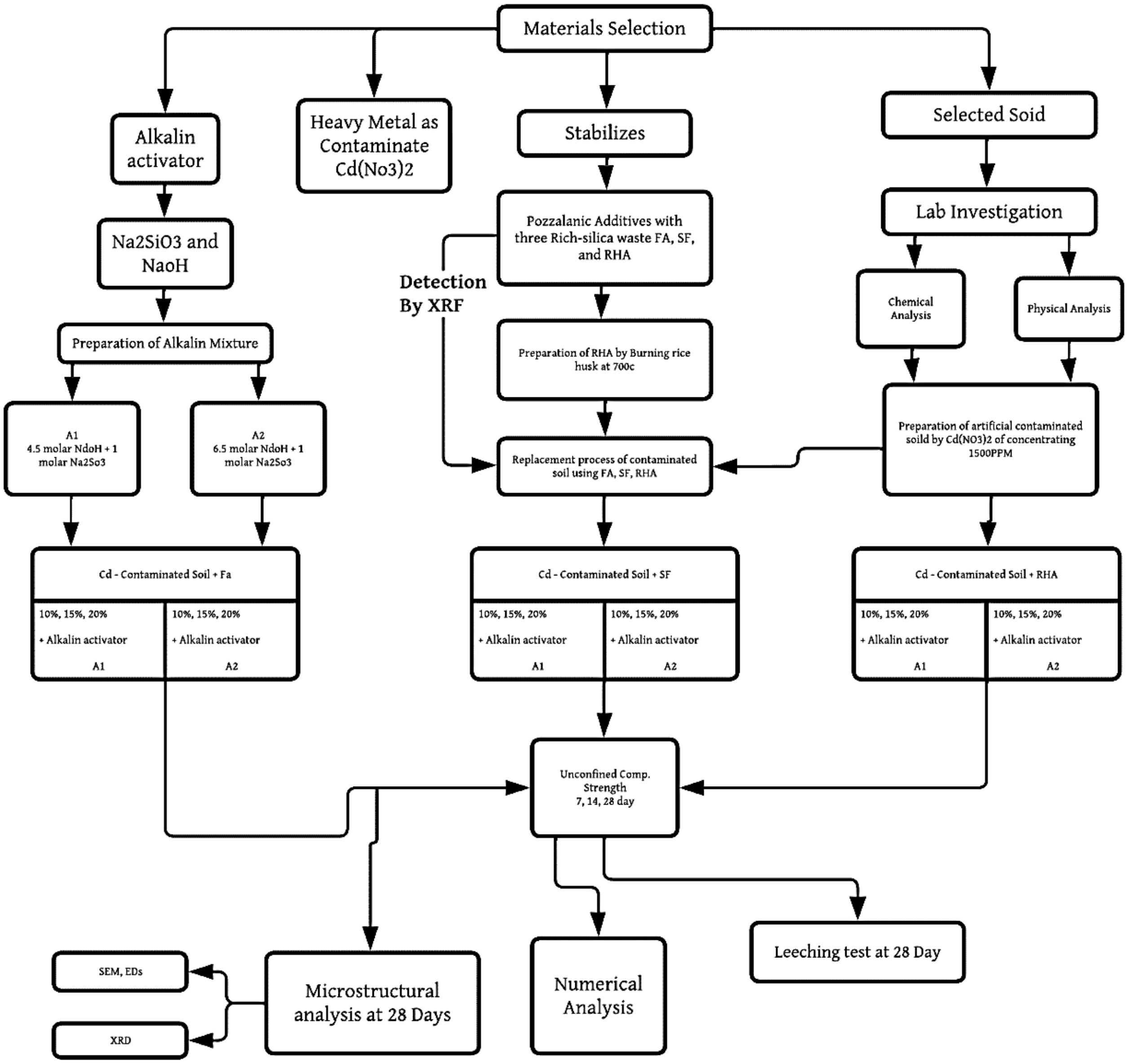

Figure 1. Research Methodology

The alkaline activator solution was prepared by mixing sodium silicate (Na_2SiO_3) and sodium hydroxide (NaOH). The sodium silicate solution was used for analysis to obtain 1 mol. NaOH with two concentrations of 4.5 mol and 6.5 mol were initially prepared. The dissolved Na_2SiO_3/NaOH ratio was adjusted by weight to two as a higher ratio provides a higher level of hardening and a lower silicate cost than hydroxide [21]. Details of the two mixing designs of the alkaline activator solution are given in Table 3. The concentrations in this table were prepared by mixing 1 kg of Na_2SiO_3 with 0.5 kg of 4.5 molar NaOH in a 2000 ml volumetric flask and stored for 24 hours to eliminate the temperature increases due to the oxidizing agent between silicate and hydroxide. A predetermined amount of alkaline activator was added, which is 20 % of the total dry weight solid (soil: ash) for all mixing processes due to (18% OMC +2% for evaporation losses).

Table 2. Types of Alkaline activator mixture

Alkaline Activator Group number	Sodium silicate concentration	Sodium hydroxide concentration
A1	1 Molar	4.5 Molar
A2	1 Molar	6.5 Molar

Stabilized Cadmium-contaminated specimens mixed with the Alkaline Activator were prepared at different percentages, as in Table 4. This table shows that the soil and the three silica were replaced to prepare these samples. The method of preparing these specimens was by compacting them into three layers into a cylindrical mold (38 mm in diameter and 76 mm in length), then extracting and wrapped with plastic wrap and aluminum foil to prevent moisture loss. The compacted specimens were stored in a temperature-controlled room at 25°C and left to cure for 7, 14, and 28 days. In total, 54 compacted specimens were prepared. Colored labels indicated the type of binder mixed with the contaminated samples. The letters in the designation of the sample indicate the name and percentage of the binder, the concentration of sodium hydroxide, and the curing time.

The strength of hardened/stabilized specimens was assessed using the unconfined compressive strength (UCS) tests following British standards [24]. For Polluted soil, it is important to remember that the purpose of the (UCS) test was to detect the existence of hardened soil. Tests were conducted on hardened samples to determine if the treated soil was robust enough to tolerate overburden pressure. The permissible value of the strength of the landfill for disposal is 0.36 MPa to avoid compression force.

Table 3. Mixing proportions of specimens

No.	Sample Name	Sample Description (Soil %: Stabilizer %) - (NaOH Concentration)	Waste Binder
1	F10A1	(Soil90:FA10)-(4.5 molal:1 Molar)	Fly Ash
2	F10A2	(Soil90:FA10)-(6.5 molal: 1 Molar)	
3	F15A1	(Soil85:FA15)-(4.5 molal: 1 Molar)	
4	F15A2	(Soil85:FA15)-(6.5 molal: 1 Molar)	
5	F20A1	(Soil80:FA20)-(4.5 molal: 1 Molar)	
6	F20A2	(Soil80:FA20)-(6.5 molal: 1 Molar)	
7	S10A1	(Soil90:SF10)-(4.5 molal: 1 Molar)	Silica fume
8	S10A2	(Soil90:SF10)-(6.5 molal: 1 Molar)	
9	S15A1	(Soil85:SF15)-(4.5 molal: 1 Molar)	
10	S15A2	(Soil85:SF15)-(6.5 molal: 1 Molar)	
11	S20A1	(Soil80:SF20)-(4.5 molal: 1 Molar)	
12	S20A2	(Soil80:SF20)-(6.5 molal: 1 Molar)	
13	R10A1	(Soil90:RHA10)-(4.5 molal: 1 Molar)	Rice Husk Ash
14	R10A2	(Soil90:RHA10)-(6.5 molal: 1 Molar)	
15	R15A1	(Soil85:RHA15)-(4.5 molal: 1 Molar)	
16	R15A2	(Soil85:RHA15)-(6.5 molal: 1 Molar)	
17	R20A1	(Soil80:RHA20)-(4.5 molal: 1 Molar)	
18	R20A2	(Soil80:RHA20)-(6.5 molal: 1 Molar)	

Following the strength tests after 28 days, the toxicity characteristic leaching procedure (TCLP) was used to evaluate the stabilization's performance. All sample was filtrated through a No. 40 sieve (0.425μm) before the TCLP tests. Five grams of crushed stabilized sediment, further ground to the finest particles passing 425m in a Ball mill, was deposited in 500-mL plastic bottles and combined with 100mL of TCLP extraction fluid. A liquid acceptable for extraction was acetic acid (pH 2.88), with a (solid-to-liquid) ratio of 1:20 by weight of the sieved material. The TCLP procedure added 5.67 ml of acetic acid to 1 L of deionized water to prepare this liquid. The mixture was then transferred to a batch mixer, digital variable speed mixer CF-1, as shown in Figure 2, for 24 hours at 30 rpm rotation speed, as shown in Figure 3.

Figure 2. Batch Mechanical Stirrers

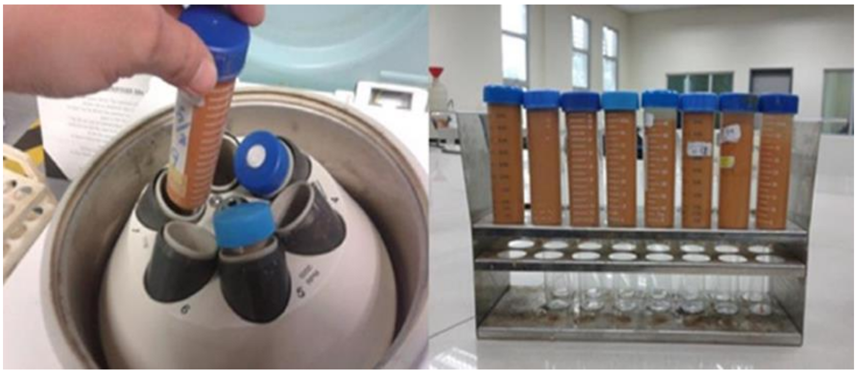

Figure 3. Sample preparation for centrifuging

A membrane filter with a pore size of 0.45 µm filters the leachate. Since metals remain dissolved at a pH less than 2.0, the pH of the leachate was decreased to less than 2.0 after filtration to minimize metal precipitation before metal analysis by adding a few drops of nitric acid [6]. The extracted liquid was retained for atomic absorption lead analysis.

The mineralogy and morphology investigation was done to indicate the cementitious phase and minerals that are responsible for the effectiveness of the stabilization process for contaminated soils [21, 23, 25]. Solidified samples were grounded into a fine powder and passed through a No.200 sieve for XRD analysis. After the samples were put within an aluminium holder, they were evenly compressed until a smooth surface emerged. A Shimadzu X-Diffractometer, with angle scan 2 theta started from 10 to 80 degrees and a step rate of 0.02 degrees/per second, was used for the mineralogical scan. The results of mineralogy were analyzed as described in the standard [26]. The change in morphological and topographic characteristics of the clay particles was studied by the Silicon Drift Detector (SDD) X-Max. A 10000X magnification SEM picture was acquired for the control and solidified samples. For proper scanning electron microscopic analysis, all samples were dried to avoid water evaporation during the tests in a vacuum environment, and electrons were utilized to produce the SEM image.

3. Numerical Analysis

3.1. Failure criteria

The strength of soils is one potential failure criterion representing engineering materials. Conical failure criteria, of which the Mohr-Coulomb criterion is unquestionably the most well-known, are applicable for soils with both frictional and cohesive components of shear strength. Cylindrical failure criteria are applicable and are covered first for metals or undrained clays that behave "frictionlessly" ($\varphi u \approx 0$).

3.2. Von Mises

This criterion assumes the shape of a right circular cylinder positioned along the space diagonal, as seen in Figure 4. When assessing whether a stress state has reached the limit of elastic behavior, only one of the three invariants, t or $\bar{\sigma}$ Is significant. A von Mises material's onset of yield is independent of the invariants s or θ. When seen in the π Plane, the von Mises criterion is symmetric, which explains why correlations with conventional soil mechanics ideas of strength are not well expressed by it. Since the criterion provides equal weight to all three principal stresses, the value of the intermediate principal stress, σ_2, After failure, it must be considered if it is to be used to describe the behavior of undrained clay.

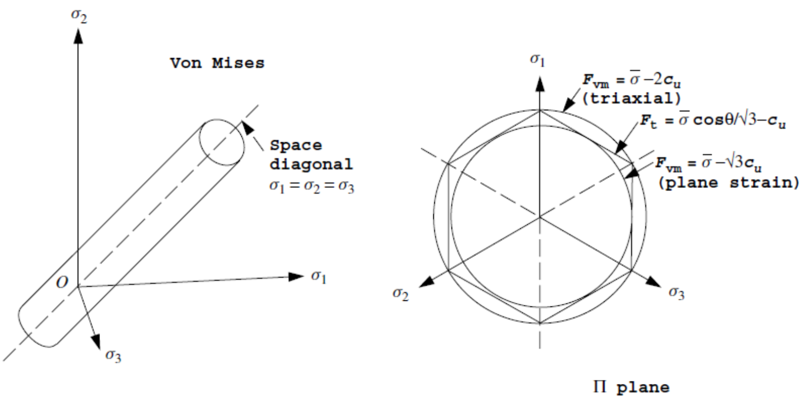

Figure 4. Failure criteria for Von Mises and Tresca [27]

It can be demonstrated that there is no plastic volume change at failure for applications involving plane strain.

$$\sigma_2 = \frac{\sigma_1 - \sigma_3}{2} \tag{1}$$

Consequently, the von Mises criterion stated by:

$$F_{vm} = \bar{\sigma} - \sqrt{3}\, c_u \tag{2}$$

should be applied, where c_u Represents the soil's undrained "cohesion" or shear strength. Contrarily, in triaxial circumstances, where:

$$\sigma_2 = \sigma_3 \tag{3}$$

The necessary van Mises criterion is provided by:

$$F_{vm} = \bar{\sigma} - 2c_u \tag{4}$$

Failure is guaranteed when the right stress condition is used with both phrases.

$$\left|\frac{\sigma_1 - \sigma_3}{2}\right| = c_u \tag{5}$$

3.3. Finite Element Analysis

The stabilized contaminated soil samples were used in the finite element parametric study to analyze the bearing capacity problems. Figure 5 shows the strip footing above the homogenous isotropic undrained clay soil. The footing was loaded under uniform stress (q) and increased to failure incrementally. The Von Mises failure criteria were utilized to model the undrained clay. A nonlinear finite element program presented by Smith et al. [27] Was employed in this parametric study. Figure 4 also illustrates the boundary condition and the finite element mesh of the typical bearing capacity problem.

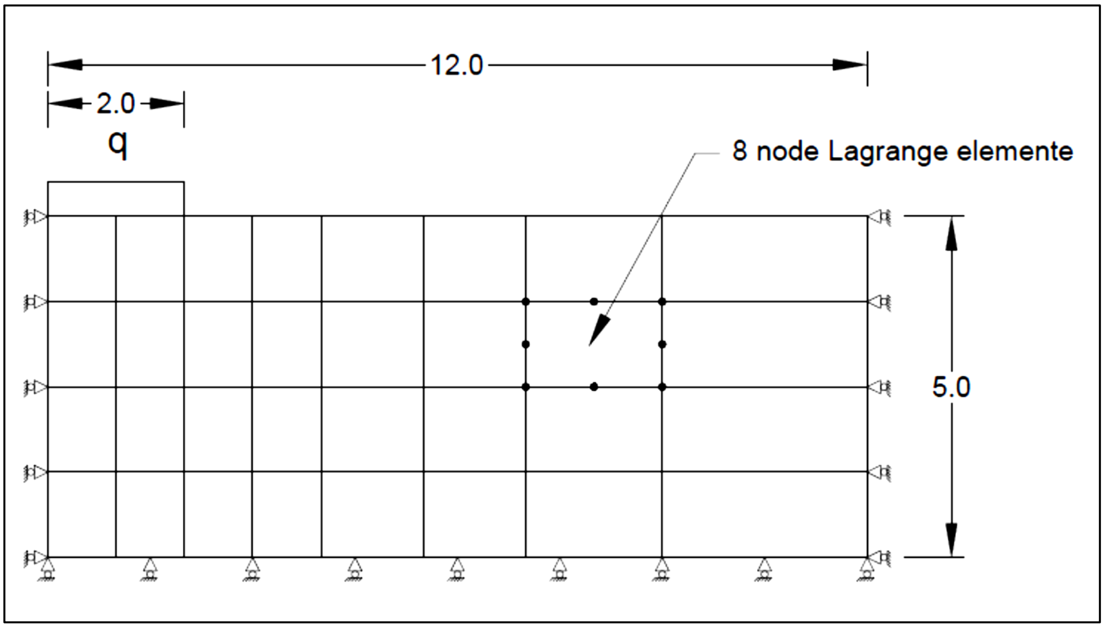

Figure 5. The boundary condition and the finite element mesh

4. Experimental Results and Discussion

Figure 6 shows the values (UCS) of samples treated with (10%, 15%, and 20 %) fly ash and activated with the alkaline solution of 4.5 and 6.5 molar obtained after 7, 14, and 28 curing days. As compared to the untreated sample (i.e., the control sample), the treated samples significantly improved, according to the results. This is because NaOH dissolves the silica and alumina in the materials, and Na_2SiO_3 binds the monomers and speeds up the geopolymerization process, which is why NaOH + Na2SiO3 performs better. This explains the notable strength enhancement for these mixes. [24, 28].

The sodium hydroxide concentration plays a significant role in soil strength, in which all samples activated by 6.5 alkaline solution (A2) exhibited higher strength than those samples activated by 4.5 alkaline solution (A1) and met the minimum landfill disposal limit of 0.36 N/mm^2 (360 kPa). The highest increase in the UCS was by 220 kPa for specimen F10A1 in group A1 and by 1200 kPa for specimen F20A2 in group A2. The UCS of mixtures activated with 4.5 molars decreased within 100 kPa with increasing fly ash contents and curing period. Similarly, increasing percentages of fly ash in the mixtures activated with 6.5 molars caused a decrease in the UCS values. However, a longer curing period enhanced the strength of A2 groups except for specimen F15A2. After 14 days of curing, the maximum obtained strength was attained by specimen F10A2. Meanwhile, specimen F20A2 showed a much higher strength of 450 kPa after 28 days of curing. This behavior is agreed with Parhi et al. [28], which can be related to the required period for the nucleation phase, during which the products result from the dissolution of raw silica and alumina before precipitation. Moreover, the low rate of Si and Al release in FA is the cause of the low strength gain in mixtures during the early phases of curing [4].

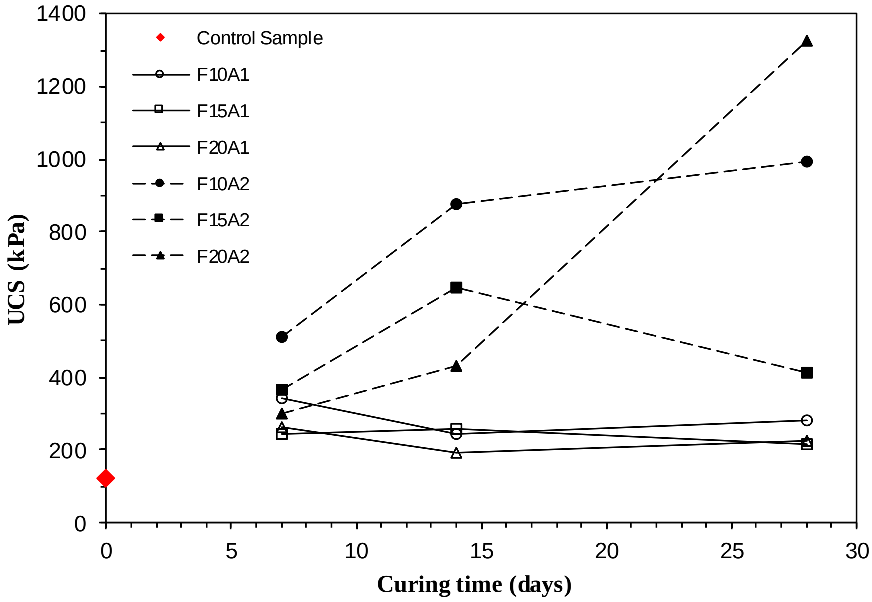

Figure 6. Unconfined compressive strength of treated specimens with fly ash versus the curing period

Figure 7 shows the changes in (UCS) values with the curing period of specimens stabilized with different percentages of silica fume and activated with 4.5 and 6.5 mol of alkaline solutions. The results revealed an improvement in the strength of treated specimens compared to the polluted sample. Rich silica and Ca are added to the system, causing calcium silicate hydrate (CSH) gels to form, which accounts for this notable improvement. Ca can also be replaced by Na or K to create calcium aluminosilicate hydrate (CASH) gels in geopolymeric gels, sodium aluminosilicate hydrate (NASH), or potassium aluminosilicate hydrate (KASH) gels. Through their joint impact on strength development, CSH, and NASH gels coexist in the system [3].

Generally, the longer the curing duration, the higher the exhibited strength of specimens at a given silica fume content. However, no clear trends in strength behavior can be noticed when the silica fume content increases and the curing period is prolonged. For specimens with 4.5 molar of NaOH and curing day 7, the maximum strength was found at specimen (S10A1). With a curing time of 14 days, 20% of silica fume specimens showed the highest strength (S20A1). However, the strength fluctuated over a longer curing period. Among 6.5 molar specimens and 7 days of curing, the maximum UCS was obtained at 20% silica fume, while the 15% silica fume specimen had a higher strength. From these results, it can be concluded that the maximum U CS values were obtained from the specimen (S20A2) after a week from the specimen (S20A1) after about 2 weeks and from the specimen (S15A2) after about 4 weeks of curing. This variation is related to heavy metals retardation and cementitious material formation.

The effect of the alkaline activators also cannot be distinguished. Such sodium hydroxide concentrations had little effect on UCS values up to 14 days of curing. Whereas with increasing the curing period to 28 days, a clear increase in the strength of specimens in group A2.

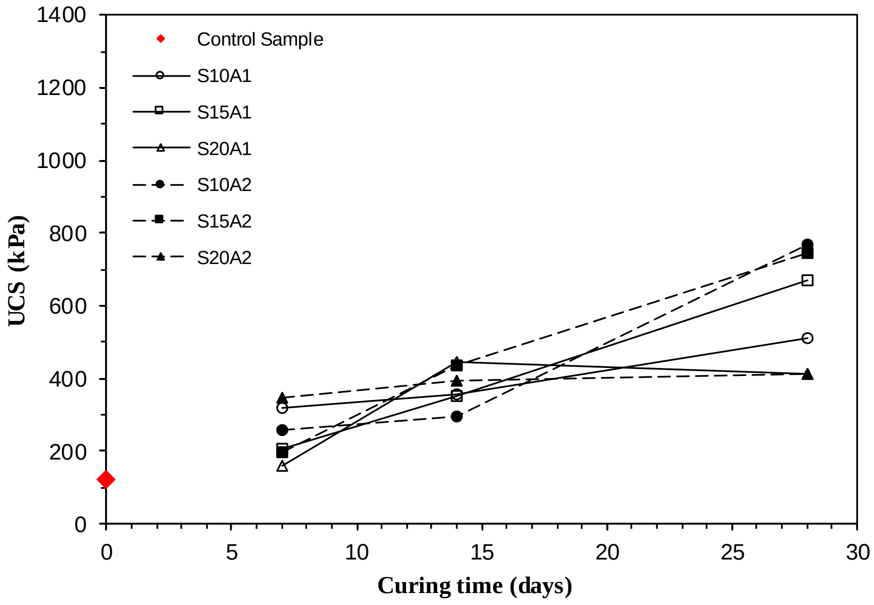

Figure 7. Unconfined compressive strength of treated specimens with silica fume versus curing period

Figure 8 shows the variation in the (UCS) values of samples treated with 10%, 15%, and 20 % rice hush ash (RHA) and activated with 4.5 and 6.5 molar of alkaline solution with curing days. The results showed increases in the unconfined compressive strength of treated specimens with increased curing time. It can be seen that the UCS of specimens activated with 4.5 molar solutions decreased with increasing the rice husk ash content, suggesting 10% as the optimum content of rice husk ash. Meanwhile, 15% of RHA had the highest strength for specimens in group A2. This behavior was in agreement with Borges et al. [29], which indicated that the systems strength had significantly changed due to the high SiO_2 in it.

The effect of increasing the sodium hydroxide concentration on the gained strength was also evident from the results. The specimens with 6.5 molars had higher strength than those with 4.5 molars.

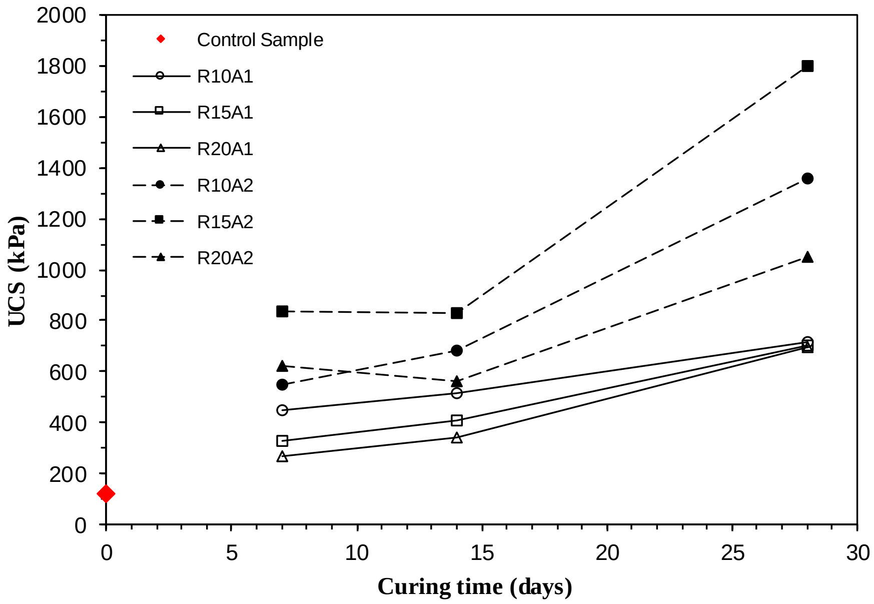

Figure 8. Unconfined compressive strength of treated specimens with rice husk ash versus curing period

Figures 9-a to 9-c present the strength development versus curing time of specimens stabilized with three rich silica additives (i.e., fly ash, silica fume, and rice husk ash) at 10%, 15%, and 20%, respectively.

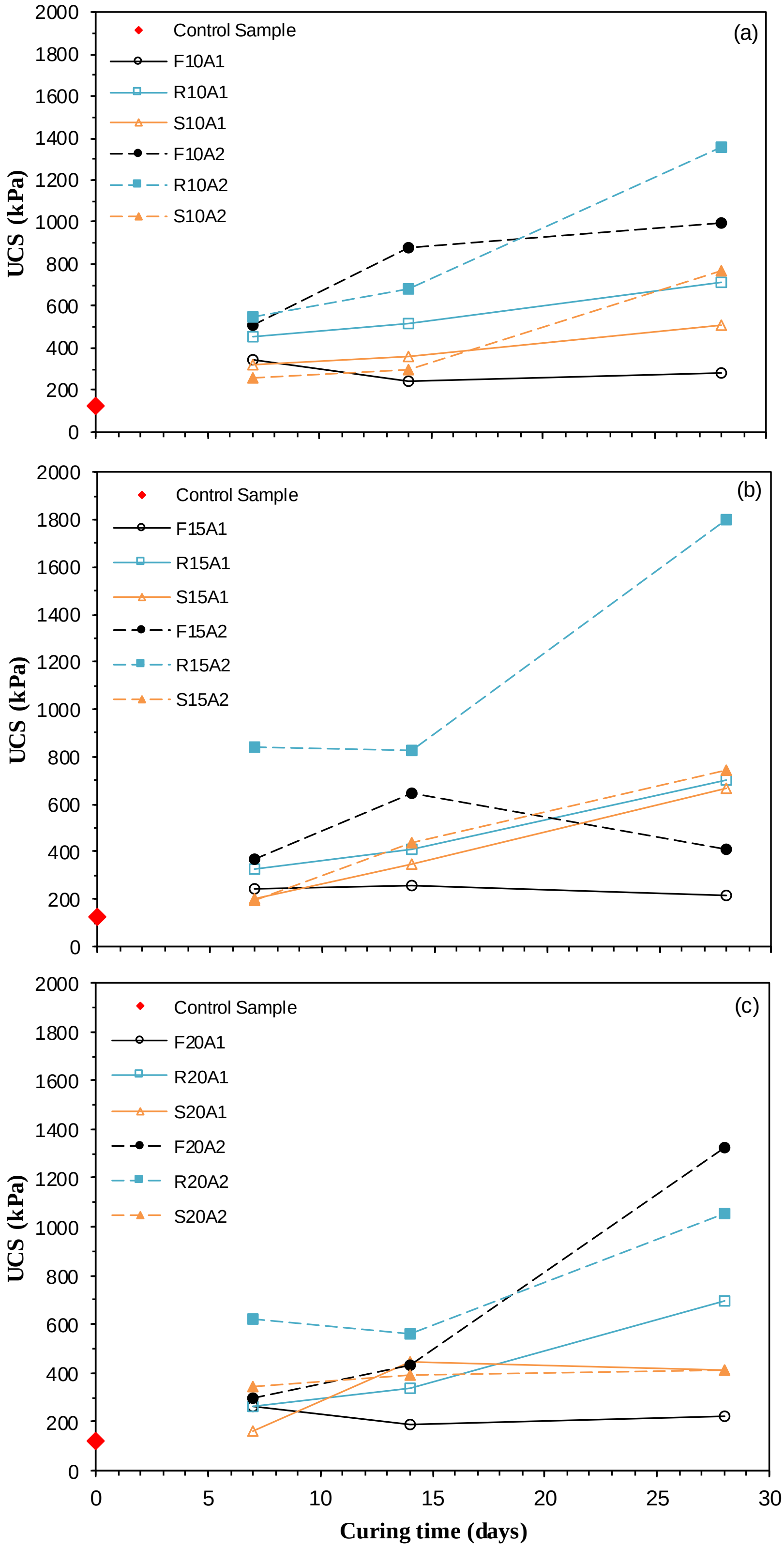

Figure 9. UCS versus curing period of treated specimens with stabilizers mixed at (a) 10%, (b) 15%, and (c) 20%

By adding 10% of different stabilizers, the attained UCS values were almost higher for specimens mixed with 6.5 molars of alkaline activator (i.e., group A2) than those in A1 with the exemption in specimen S10A2. The comparison analysis revealed that stabilizing polluted soil with rice husk ash produced the greatest compressive strength compared to fly ash and silica fume. However, the strength of specimens mixed with fly ash and cured for a week was higher than that of other binders.

Specimens stabilized with 15% binders showed similar behavior in the attained compressive strength to those stabilized with 10%. The results revealed that the best by-product waste material used to treat cadmium-contaminated soil was rice husk ash, followed by fly ash and silica fume. The strength of treated specimens using RHA increased 14 times that of the untreated specimen after 28 curing days.

At 20% addition of FA, SF, and RHA to the contaminated soil, the UCS values were higher for specimens in group A2. The rice husk ash also stabilized the polluted specimen better, increasing the unconfined compressive strength compared to the other binders. It is evident from these results that the three used rich silica additives improved the strength characteristics of the contaminated soil. However, the best improvement was reached when the contaminated soil stabilized with 15% rice husk ash.

Figure 10 shows the leached concentration of cadmium for samples after 28 days of curing, which were treated with 10%, 15%, and 20% of FA, SF, and RHA binders and activated with alkaline solutions of 4.5 and 6.5 molar. The control sample had a maximum leaching concentration of 39.2 mg/l. The cadmium content in the cured samples was lower than in the polluted samples and remained above the EPA leachability limit (5 mg/l). This shows that alkali-activated aluminosilicate materials are very effective at immobilizing cadmium ions and transforming dangerous slag into safe building materials for humans and the environment. This may be due to the low solubility of its hydroxide product in addition to these contaminants' strong capacity to adsorb on the surface of the geopolymer's hydration products, particularly the CSH and CASH phases [5, 21]. Among samples treated with fly ash, the cadmium concentrations of samples with 4.5 molars were higher than those with 6.5 molars. The highest treatment efficiency of 83 % was achieved by the specimen (F10A2), and the lowest treatment efficiency of 67.9 % was obtained with the specimen (F20A1).

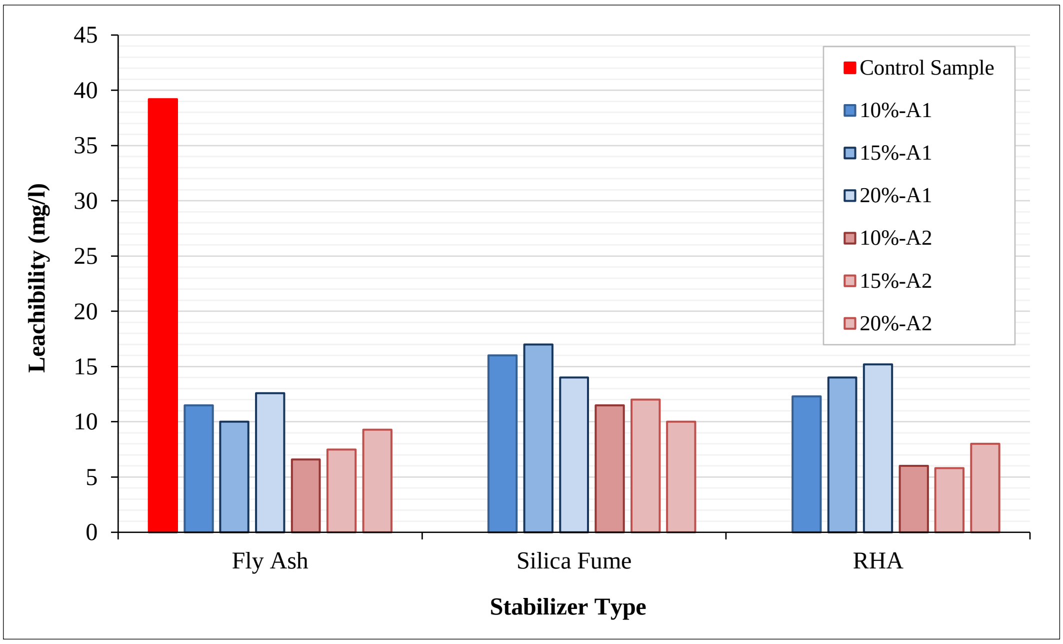

Figure 10. Leaching Results for Cadmium stabilized soil using three rich silica additives

Similarly, stabilizing the contaminated samples with silica fume produced the lowest cadmium concentration in the specimen (S20A2), while the higher leachability was found with (S15A1) and treatment efficiency of 56.6%. The rice husk ash addition results indicated that the leachability rate was reduced to 5.8 mg/l with 85.8 % efficiency in the specimen (R15A2). At the same time, the lower level of treatment was obtained with specimens treated with 4.5 molars of NaOH. This is related to the high degree of immobilization with time progress. The activation process produces hydration products that stabilize and solidify heavy metals [29].

The results of the TCLP leaching test indicated that RHA achieved the highest treatment efficiency with 85.8% at mix ratio (R15A2), followed by FA at mix ratio (F10A2) with 83%, then SF which attained the lowest treatment efficiency of 74.5% at mix ratio (S20A2). It also showed that sodium hydroxide concentration significantly reduces the leachability rate among all the lead-solidified samples. These results were in agreement with those of Khan et al. [6], who believed that hydroxide precipitation was responsible for the effective treatment. However, the low solubility of heavy metal hydroxide products and the high ability to adsorb cadmium ions on the surface of hydration products may cause this [30].

Figure 11 shows the pH levels of stabilized and solidified samples at 28 days of curing. The results showed that the PH of the control sample was 7.55 after increasing the polymerization process range from 11.2 to 11.46. The pH levels of specimens at different binder contents almost reached an equivalent value of 11.35 with little increment when using 6.5 molars of NaOH. The decreased pore size and matrix permeability could be the main factors lowering the leachability of cadmium.

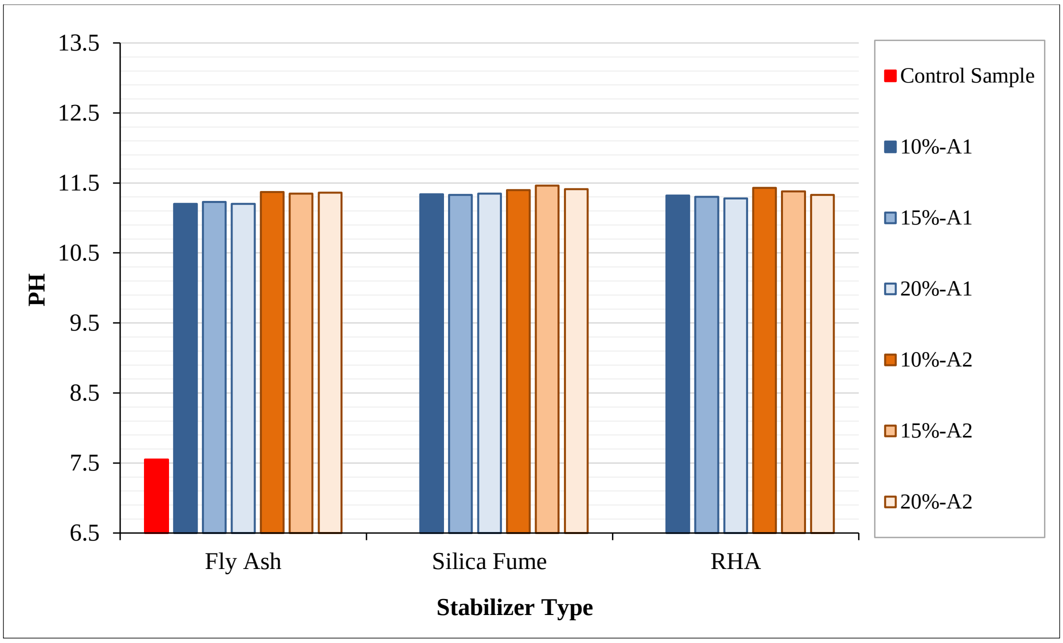

Figure 11. pH Analysis of Stabilized Soil using three rich silica additives

Another reason for lead immobilization is the formation of precipitates in geo-polymeric matrices, which could be either metal hydroxide or silicate species. Therefore, the metal immobilization was thought to depend strongly on the alkali activators pH [30]. It was also discovered that when the solutions pH rose, the adsorption on geopolymers increased, which led to an increase in the adsorption capability of heavy metals.

Figures 12-a to 12-c, and d illustrate the XRD results of the contaminated soil stabilized by adding by-product wastes and an alkaline activator. Major minerals present in naturally contaminated soil are shown in Figure 12-a, including silicon sulfide, Quartz, and Clinoferrosilite, in addition to the cadmium compounds like cadmium oxide, cadmium silicate, and cadmium oxide sulfate (Lanarkite). Figure 12-b shows the minerals formed after stabilization with fly ash and 6.5 molar activators. Silicon Sulfide, Sodium Silicate, Nickel Carbide, and silica were found in the treated specimen (F20A2). No cadmium peaks were detected within fly ash stabilized soil as an indicator for the curing process of Cd^{+2}. Not only relies on the precipitation process and may depend on the adsorption process or encapsulation during the curing time, as Xi et al. [31] observed when replacing diatomite with cement for solidifying the Cd-contaminated soil. The presence of nickel carbide is related to the impurities within the fly ash.

Figure 12-c shows the minerals formed after stabilization with SF in the specimen (S15A2). Quartz, Sodium silicate, Silicon Sulfide, Calcite, Nickel Carbide, and Calcium Oxide were found at XRD peaks. Sodium silicate was found at 2ϴ (26.5 and 47.5) as a gel formation for the cementitious compound. Figure (12d) displays the minerals formed after stabilization with RHA in the specimen (R15A2). The major compounds detected by XRD were calcite and silicon sulfide.

Calcite, found at SF and RHA, is related to the carbonation of calcium due to the exothermic reaction of alkali-activated and weak cementitious compounds such as calcium carbonate. The formation of calcite is induced by the interaction between (OH-) for the alkaline activator and Ca2+ for the source material of the specimen to create calcium hydroxide Ca (OH)2, which later reacts with CO2 in the atmosphere [32]. These are dehydrated strength-giving phases like calcium silicate hydrate (CSH) and calcium aluminum silicate hydrate (CASH). Saeed et al. [25] The cementitious compound, which represents the heart of concrete, was detected by XRD for up to 100 days at little peaks in the presence of heavy metals. This observation proved that heavy metals can retard the formation of C2S and C3S at the early stages of curing. Fernández-Jiménez & Palomo [32]: another important observation is that the calcium content present in each binder affects the C-S-H gel formation. All the binders used were considered to have low calcium content. Therefore, the geopolymerization process mostly yielded on the Si-O-Al and Si-O-Si gels and needed a longer curing period to form and crystallize enough to be detected by an X-ray diffractometer. Moon & Dermatas [33] Studied lead leachability from stabilized soil through semi-dynamic leaching conditions and observed that the immobilization was caused by forming lead silicate (PbSiO3) and precipitating within the solidified matrix. In the present study, XRD detected none of the lead components. Similar behavior was reported by Muhammad et al. [12] Due to the content underlies 5%. García-Lodeiro et al. [34] I thought the zeolite framework within the geopolymeric matrix could be locked in the heavy metals with superior mechanical characteristics and durability.

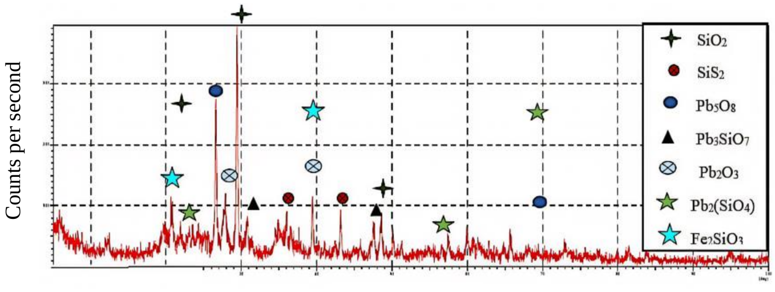

(a) CS

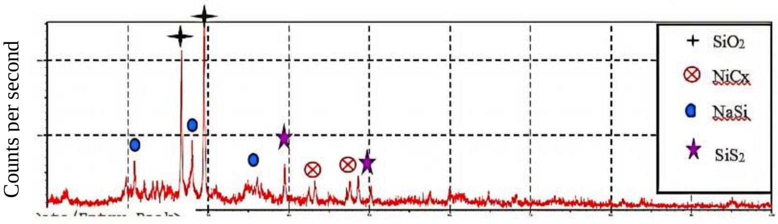

(b) F20A2

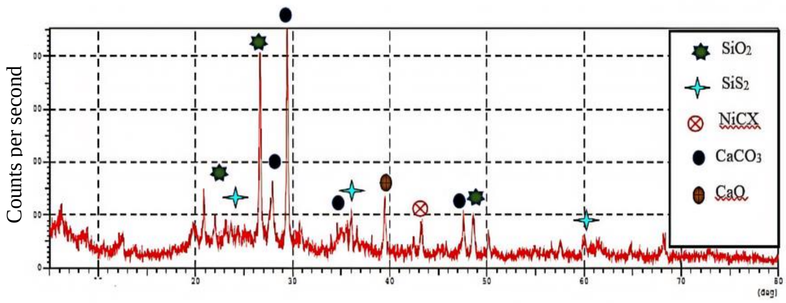

(c) S15A2

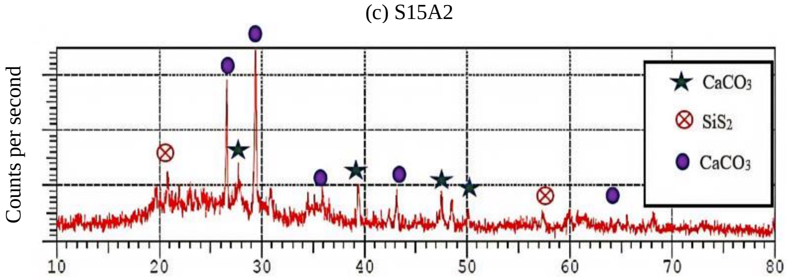

(d) R15A2

Figure 12. XRD Analysis of stabilized soil using waste materials a) Control sample, b) FA, c) SF, and d) RHA

For scanning electron microscopic analysis, Figures 13-a to 13-c, and d illustrate the SEM Image of the stabilized soil, which showed improved strength through the addition of additives and alkaline activator. A micrograph of natural silty clay soil is presented in Figure 13-a. As indicated by XRD analysis (calcium oxide, silicon oxide, and lead oxide), free oxides were found within its microstructure, coated and embedded with clay particles in the scattered composition. This result was similar to the study of Saeed et al. [23, 35].

Figure 13-b presents the morphology of specimen F20A2 stabilized with 20% fly ash and 6.5 molar NaOH. As cementitious compounds form, the image demonstrated how the soil fabric changes to a more flocculated texture and flaky look with white lumps. The porous microstructure is related to the ratio of (SiO2/Al2O3). However, this structure is denser and more homogeneous at a higher ratio of (SiO2/Al2O3) as observed by Steveson & Sagoe-Crentsil [36]. Figure 13-c shows the microstructures of stabilized soil with silica fume (S15A2) and 6.5 molar sodium hydroxide. The material appears denser, which suggests improved hydration and solidification efficiency for lead-contaminated soil. This is agreed well with the observation of Li et al. [37] while studying the development of surface morphology with and without the addition of silica fume, which can fill the micro-cracks with some stiffness.

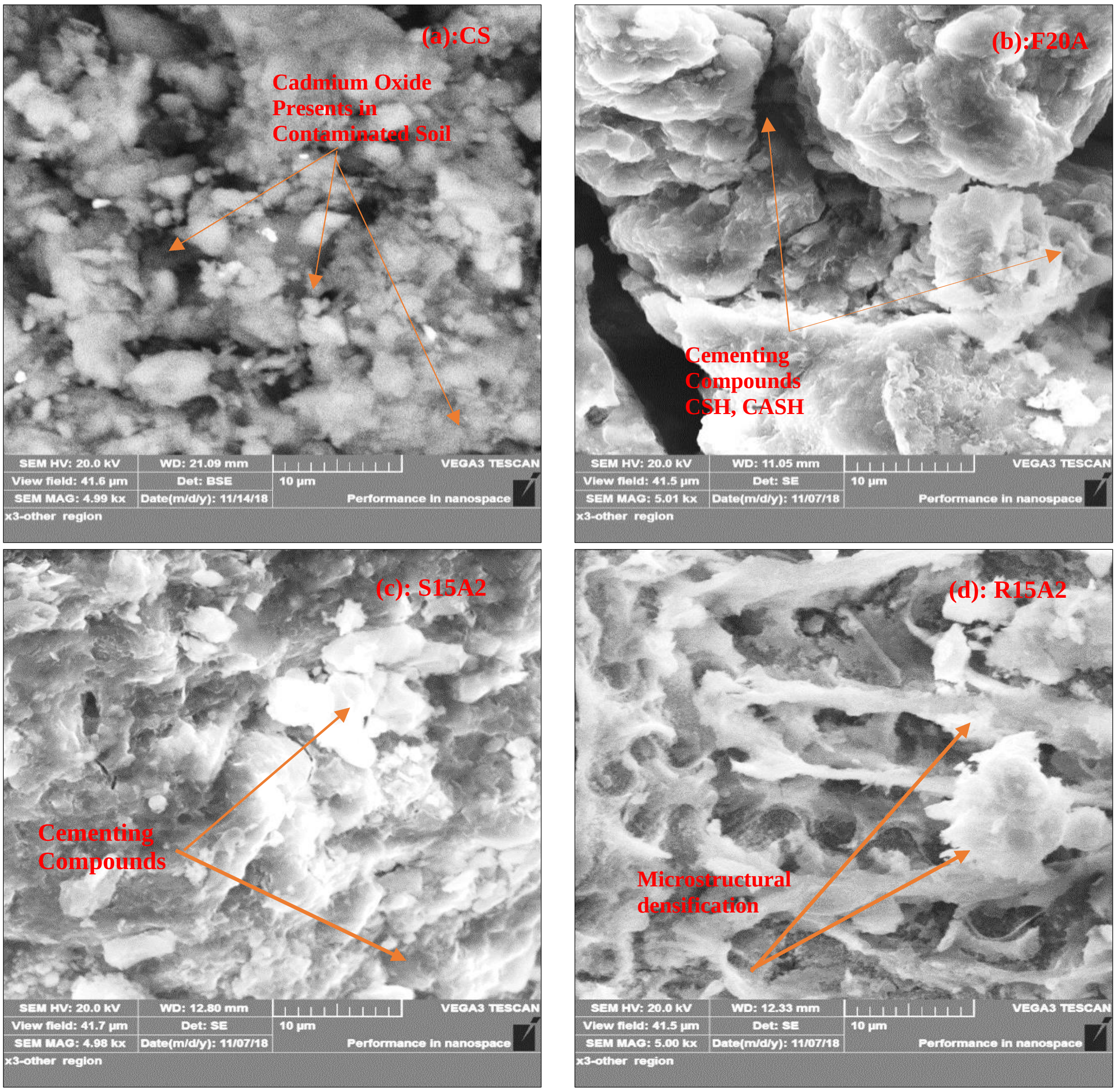

Figure 13. SEM analysis of Stabilized Soil: a) Control Sample, b) FA, c) SF, and d) RHA

Figure 13-d shows the solidified soil when replaced by 15 % of RHA and activated by a 6.5 molar NaOH solution. It can be seen that the texture transformed clay particles into the framework, which was flocculated with some flaky parts as an indicator for converting the dissolved rich silica and alumina to the hardening geopolymer matrices. Sturm et al. [38] identified the same behavior when using rice husk ash in geopolymer concrete, which exhibited the homogenous microstructure during cured conventional geopolymers.

In summary, the morphological results of silty clay soils treated with FA, SF, and RHA revealed the same formation for a cementitious compound with variations in homogeneity and porous structure connected to the reactive silica present in each binder. As a result, these distinctions help to explain why each solidified soil binder has different strengths and leaching characteristics. Furthermore, no cadmium components were found in the morphology of the solidified soil, demonstrating that the cadmium compounds may precipitate and enclose themselves inside the matrix of a rich silica cementitious framework.

5. Numerical Results and Discussion

Figures 14 to 16 show the load-settlement curves of the untreated and treated contaminated soils for 7, 14, and 28 days, respectively. The results regarding the bearing capacity ratio (BCR) and settlement reduction percentage (Rs) were analyzed. The two non-dimensional parameters are defined as follows:

$$BCR = \frac{q_{ult\ of\ treated\ soil}}{q_{ult\ of\ untreated\ soil}} \quad (6)$$

$$Rs = \frac{s_{ult\ of\ untreated\ soil} - s_{ult\ of\ treated\ soil}}{s_{ult\ of\ untreated\ soil}} \times 100 \tag{7}$$

where q_{ult} is the ultimate bearing capacity of soils and s_{ult} is the settlement at ultimate bearing capacity.

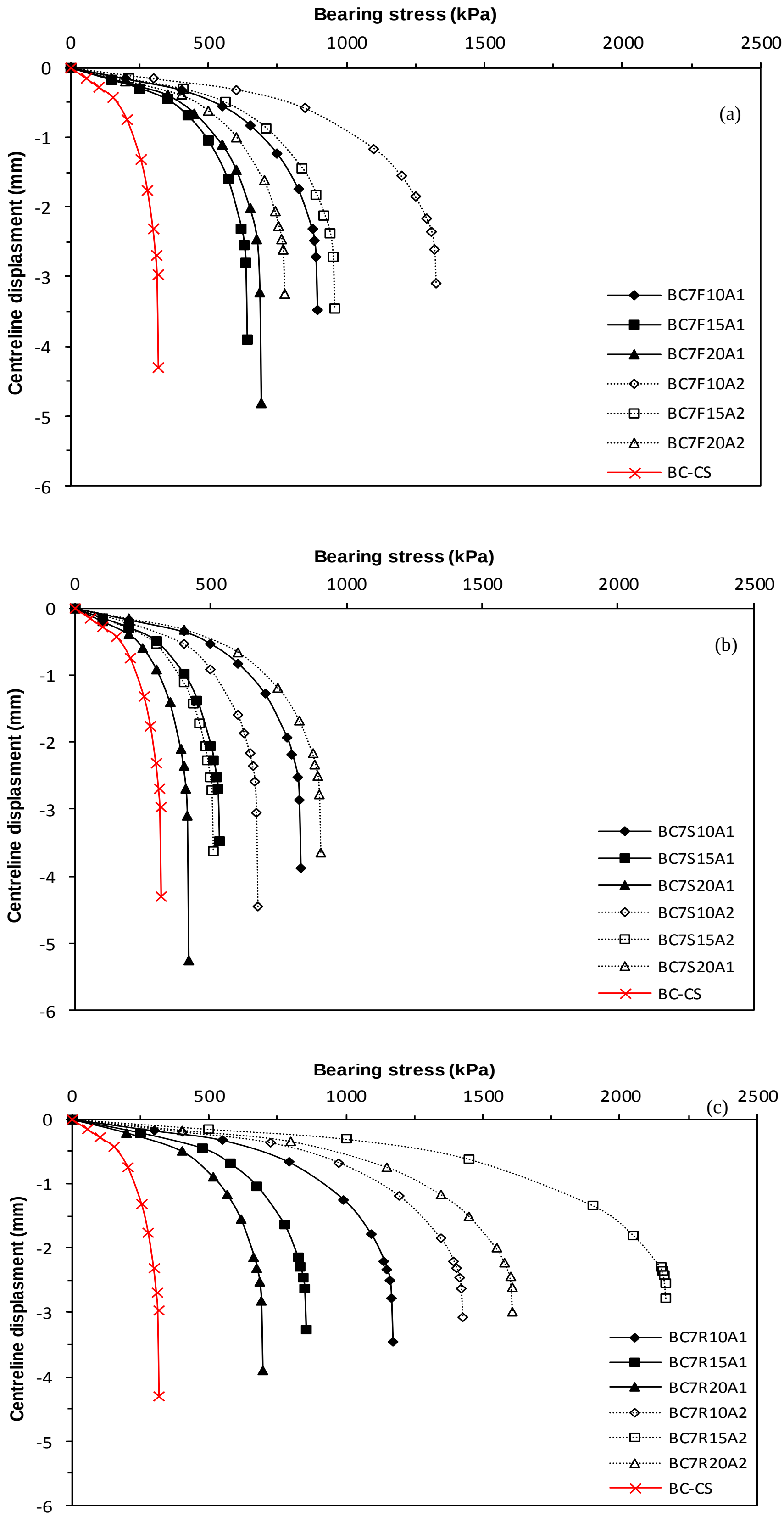

Figure 14. Load-settlement curves of samples after 7 days of curing using (a) Fly ash, (b) silica fume, and (c) Rice Husk Ash

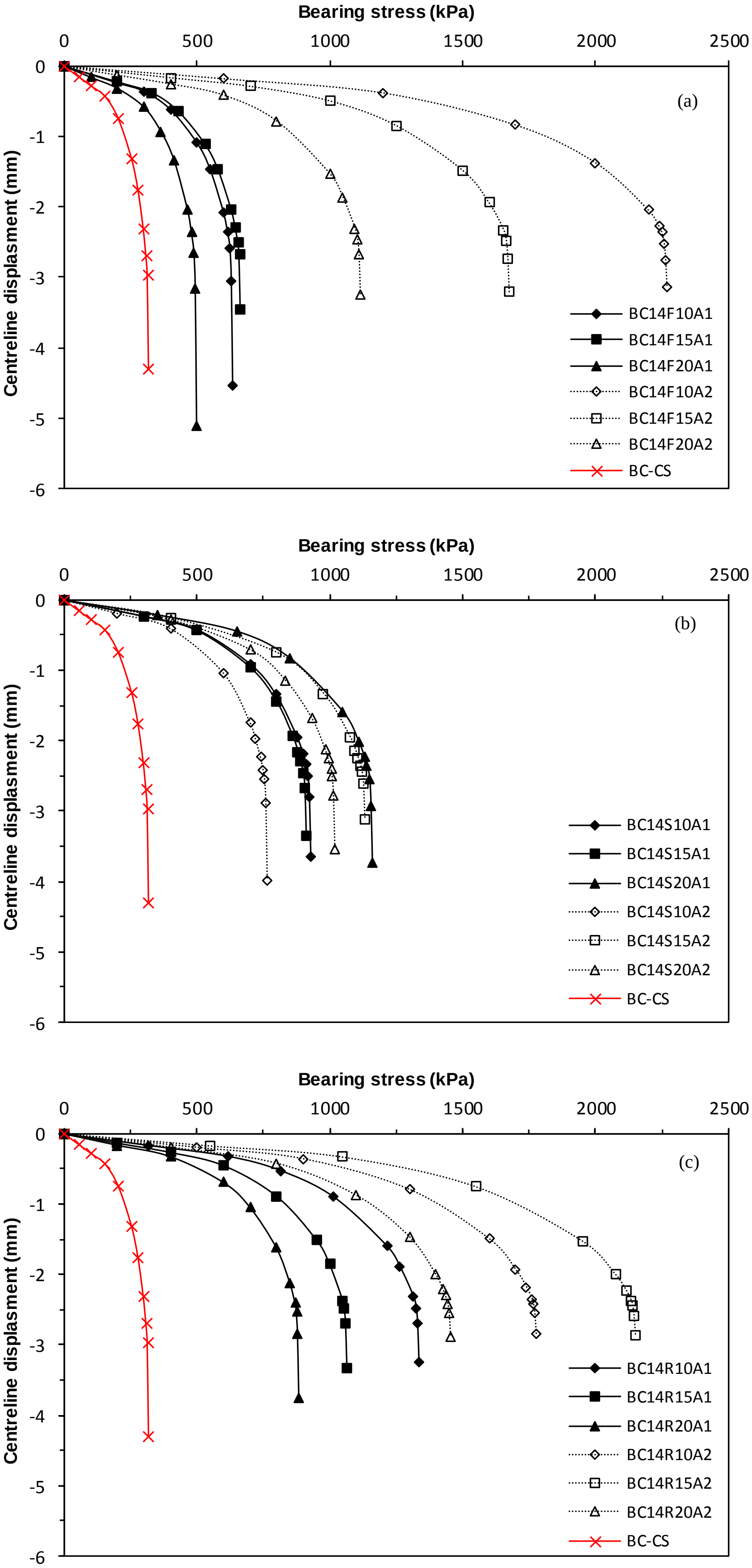

Figure 15. Load-settlement curves of samples after 14 days of curing using (a) Fly ash, (b) silica fume, and (c) Rice Husk Ash

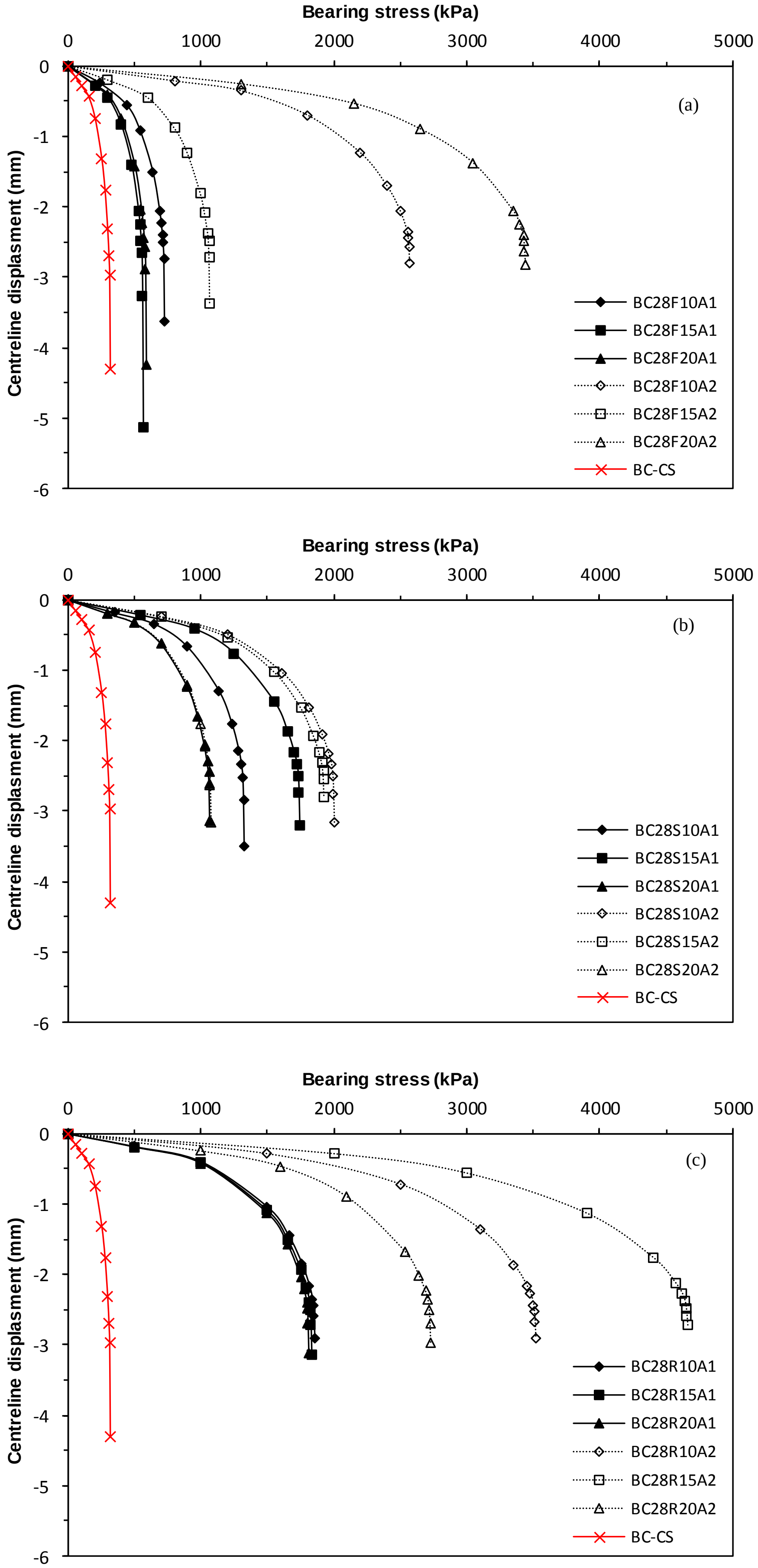

Figure 16. Load-settlement curves of samples after 28 days of curing using (a) Fly ash, (b) silica fume, and (c) Rice Husk Ash

The evaluation of ultimate bearing capacity was conducted according to the criteria suggested by Vesic [39], which defines the ultimate load as the point where the slope of the load settlement curve first reaches zero or a steady minimum value. Table 5 presents the *BCR* and *Rs* % of all the tested soil samples. Adding stabilizers and activators improves the contaminated soil's behavior by increasing the bearing capacity and reducing its settlement, as given in Table 5. The bearing capacity ratio reaches its maximum value of 6.9 in sample R15A2 after 7 days of curing, 7.2 in sample F10A2 after 14 days, and 14.8 in sample R15A2 after 28 curing time. The highest reduction in settlement was also obtained in contaminated soils stabilized by rice husk ash and activated by 6.5 mol of alkaline activators.

Table 4. Bearing capacity ratio and settlement reduction of all specimens

No.	Waste Binder	Sample Name	7 days		14 days		28 days	
			BCR	Rs (%)	BCR	Rs (%)	BCR	Rs (%)
1	Fly Ash	F10A1	2.8	9.4	2.0	-1.5	2.3	9.0
2		F10A2	4.2	12.8	7.2	8.7	8.1	14.2
3		F15A1	2.0	7.0	2.1	12.4	1.8	-9.0
4		F15A2	3.0	9.7	5.3	10.0	3.4	14.1
5		F20A1	2.2	-7.1	1.6	-4.9	1.8	3.9
6		F20A2	2.4	12.8	3.5	12.5	10.9	12.7
7	Silica fume	S10A1	2.6	4.7	2.9	6.9	4.2	5.3
8		S10A2	2.1	-1.5	2.4	4.0	6.8	8.4
9		S15A1	1.7	10.4	2.9	11.1	5.5	8.5
10		S15A2	1.6	9.4	3.6	12.7	6.1	15.2
11		S20A1	1.3	-3.3	3.7	2.5	3.4	13.0
12		S20A2	2.9	7.1	3.2	7.6	3.4	12.6
13	Rice Husk Ash	R10A1	3.7	7.3	4.2	9.9	5.6	13.6
14		R10A2	4.5	12.3	5.6	14.9	11.1	10.7
15		R15A1	2.7	12.2	3.4	10.4	5.8	9.6
16		R15A2	6.9	15.3	6.8	13.8	14.8	14.1
17		R20A1	2.2	6.2	2.8	5.5	5.7	9.9
18		R20A2	5.1	12.9	4.6	14.9	8.7	10.5

It is also clear that there is no significant improvement in BCR and Rs% gained on using silica fume compared to other additives. In some samples, stabilization does not affect the settlement, while it increases the ultimate bearing capacity and reduces the settlement, as shown in Table 5.

6. Conclusion

Three by-product waste materials rich in silica were used with chemical additives to treat artificially Cd-contaminated silty clay soil using the stabilization/solidification technique. The effectiveness of this technique in improving the engineering properties and flexibility of the contaminated soil was evaluated by conducting unconfined compressive strength (UCS), leaching, and pH tests. X-ray diffraction and scanning electron microscope (SEM) were also performed to clarify the mechanisms responsible for heavy metal immobilization. The UCS values of Cd-contaminated silty clay specimens stabilized with pozzolanic waste materials and an alkaline activator showed enormous development over the curing period. Results of the compressive strength demonstrated a continual increase with increasing hydration ages. This is attributed to the higher rate of hydration and the formation of more hydration products, such as sodium and calcium aluminum silicate hydrate. The optimum mix ratio of each binder, which provides the maximum strength, was at 20% fly ash with 6.5 molars of NaOH, 15% silica fume with 6.5 molars of NaOH, and 15% rice husk ash with 6.5 molars of NaOH. The role of NaOH was evident in significantly enhancing the strength of Cd-contaminated silty clay soil. All the solidified samples have gained UCS values that exceeded the limit of landfill disposal (340 kPa). The TCLP leaching test performed using sodium silicate solution at 1 molar ratio showed that RHA achieved a higher treatment efficiency with 85.8% at a mixing ratio (R15A2), followed by FA at a mixing ratio (F10A2) with 83%, then SF, which reached the lowest treatment efficiency of 74.5% at a mixing ratio (S20A2). The numerical results further confirmed the efficiency of the alkaline activator on stabilized cadmium-contaminated soil by rich silica additives, as indicated by the bearing capacity ratio and settlement reduction percentage.

7. Declarations

7.1. Author Contributions

Conceptualization, K.S. and S.A.; methodology, K.S.; software, Z.A.H.; validation, K.S., S.A., and Z.A.H.; formal analysis, K.S. and S.A.; investigation, K.S.; resources, K.S., S.A., and Z.A.H.; data curation, K.S. and S.A.; writing—original draft preparation, K.S. and S.A.; writing—review and editing, K.S., S.A., and S.H.F.; visualization, S.H.F.; supervision, K.S.; project administration, S.A.; funding acquisition, K.S., S.A., and Z.A.H. All authors have read and agreed to the published version of the manuscript.

7.2. Data Availability Statement

The data presented in this study are available in the article.

7.3. Funding

The authors received no financial support for the research, authorship, and/or publication of this article.

7.4. Conflicts of Interest

The authors declare no conflict of interest.

8. References

[1] Pan, H., Shao, Y., Yan, P., Cheng, Y., Han, K. S., Nie, Z., Wang, C., Yang, J., Li, X., Bhattacharya, P., Mueller, K. T., & Liu, J. (2016). Reversible aqueous zinc/manganese oxide energy storage from conversion reactions. Nature Energy, 1(5), 1-7. doi:10.1038/nenergy.2016.39.

[2] Benavides, M. P., Gallego, S. M., & Tomaro, M. L. (2005). Cadmium toxicity in plants. Brazilian Journal of Plant Physiology, 17(1), 21–34. doi:10.1590/s1677-04202005000100003.

[3] Mutter, G. M., Al-Madhhachi, A. T., & Rashed, R. R. (2017). Influence of soil stabilizing materials on lead polluted soils using Jet Erosion Tests. International Journal of Integrated Engineering, 9(1), 28-38.

[4] Hasan, M. B., & Al-Madhhachi, A.-S. T. (2018). The Influence of Crude Oil on Mechanistic Detachment Rate Parameters. Geosciences, 8(9), 332. doi:10.3390/geosciences8090332.

[5] Al-Madhhachi, A. S. T., Mutter, G. M., & Hasan, M. B. (2019). Predicting Mechanistic Detachment Model due to Lead-Contaminated Soil Treated with Iraqi Stabilizers. KSCE Journal of Civil Engineering, 23(7), 2898–2907. doi:10.1007/s12205-019-2312-3.

[6] Khan, M. A., Khan, S., Khan, A., & Alam, M. (2017). Soil contamination with cadmium, consequences and remediation using organic amendments. Science of the Total Environment, 601–602, 1591–1605. doi:10.1016/j.scitotenv.2017.06.030.

[7] Charyulu, S. V., Akhila, C., Vineetha, Ch., & Akanksha, A. (2023). Stabilisation of soil using rice husk ash (RHA) and cement. E3S Web of Conferences, 391, 01201. doi:10.1051/e3sconf/202339101201.

[8] Arbili, M. M., Karpuzcu, M., & Ali, M. M. (2020). Impact of Silica Fume on the Strength Characterizes of Contaminated Soil. Polytechnic Journal, 10(1), 6–11. doi:10.25156/ptj.v10n1y2020.pp6-11.

[9] Hadi, N. S., Awadh, H. H., & Khalil, A. H. (2022). Experimental Study for the Effect of Additives Silica Fume on the Properties of the Synthetically Contaminated Soil. Environmental Research, Engineering and Management, 78(1), 46–56. doi:10.5755/j01.erem.78.1.29869.

[10] Ramezani, S. J., Toufigh, M. M., & Toufigh, V. (2023). Utilization of Glass Powder and Silica Fume in Sugarcane Bagasse Ash-Based Geopolymer for Soil Stabilization. Journal of Materials in Civil Engineering, 35(4), 4023042. doi:10.1061/(asce)mt.1943-5533.0004704.

[11] Lin, J., Zhang, Y., & Yang, Z. (2023). A Review of Recent Advances in Alkali-activated Materials from Silica-rich Wastes Derived Sodium Silicate Activators. Journal of Advanced Concrete Technology, 21(3), 189–203. doi:10.3151/JACT.21.189.

[12] Muhammad, F., Huang, X., Li, S., Xia, M., Zhang, M., Liu, Q., Shehzad Hassan, M. A., Jiao, B., Yu, L., & Li, D. (2018). Strength evaluation by using polycarboxylate superplasticizer and solidification efficiency of Cr6+, Pb2+ and Cd2+ in composite based geopolymer. Journal of Cleaner Production, 188, 807–815. doi:10.1016/j.jclepro.2018.04.033.

[13] Cristelo, N., Glendinning, S., Miranda, T., Oliveira, D., & Silva, R. (2012). Soil stabilisation using alkaline activation of fly ash for self-compacting rammed earth construction. Construction and Building Materials, 36, 727–735. doi:10.1016/j.conbuildmat.2012.06.037.

[14] Wang, H., Zhu, Z., Pu, S., & Song, W. (2022). Solidification/Stabilization of Pb2+ and Cd2+ Contaminated Soil Using Fly Ash and GGBS Based Geopolymer. Arabian Journal for Science and Engineering, 47(4), 4385–4400. doi:10.1007/s13369-021-06109-1.

[15] Rios, S., Ramos, C., Fonseca, A. V. Da, Cruz, N., & Rodrigues, C. (2016). Colombian Soil Stabilized with Geopolymers for Low Cost Roads. Procedia Engineering, 143, 1392–1400. doi:10.1016/j.proeng.2016.06.164.

[16] Liu, F., Huang, X., Zhao, H., Hu, X., Wang, L., Zhao, X., Gao, P., & Ji, P. (2021). Stabilization of Cd and Pb in the contaminated soils by applying modified fly ash. Soil Ecology Letters, 3(3), 242–252. doi:10.1007/s42832-021-0078-2.

[17] Mahedi, M., Cetin, B., & Dayioglu, A. Y. (2019). Leaching behavior of aluminum, copper, iron and zinc from cement activated fly ash and slag stabilized soils. Waste Management, 95, 334–355. doi:10.1016/j.wasman.2019.06.018.

[18] Abhishek, H. S., Prashant, S., Kamath, M. V., & Kumar, M. (2022). Fresh mechanical and durability properties of alkali-activated fly ash-slag concrete: a review. Innovative Infrastructure Solutions, 7, 1-14. doi:10.1007/s41062-021-00711-w.

[19] Turan, C., Javadi, A. A., Vinai, R., & Russo, G. (2022). Effects of Fly Ash Inclusion and Alkali Activation on Physical, Mechanical, and Chemical Properties of Clay. Materials, 15(13), 4628. doi:10.3390/ma15134628.

[20] Ayila, A. A., & Ramana Murty, V. (2024). Experimental study on strength and microstructural properties of hydrous magnesium alkalization in colligation with tropical laterite soil at ambient temperature. Sādhanā, 49(1), 67. doi:10.1007/s12046-024-02435-w.

[21] Kadhim, H. J., Saeed, K. A., & Kariem, N. O. (2019). Using geopolymers materials for remediation of lead-contaminated soil. Pollution Research, 38(4), 85–95.

[22] Vosugh, S. (2001). Mechanical properties and Durability of Concretes Containing of Rice Husk Ash. PhD Thesis. Amirkabir University of Technology, Tehran, Iran.

[23] Saeed, K. A., Kassim, K. A., Nur, H., & Yunus, N. Z. M. (2015). Strength of lime-cement stabilized tropical lateritic clay contaminated by heavy metals. KSCE Journal of Civil Engineering, 19(4), 887–892. doi:10.1007/s12205-013-0086-6.

[24] BS 1377-8:1990. (1990). Methods of test for soils for civil engineering purposes: Part 8: Shear strength tests (effective stress). British Standard Institution, London, United Kingdom.

[25] Saeed, K. A., Kassi, K. A., Nur, H., & Al-Hashimi, S. A. M. (2020). Molecular Characteristics of Cement-Lime Treated contaminated-Lateritic Clay Soil. IOP Conference Series: Materials Science and Engineering, 870(1), 012082. doi:10.1088/1757-899x/870/1/012082.

[26] Joint Committee on Chemical Analysis by Powder Diffraction Methods. (1960). Powder Diffraction File. American Society for Testing and Materials, West Conshohocken, United States.

[27] Smith, I. M., Griffiths, D. V., & Margetts, L. (2013). Programming the Finite Element Method. John Wiley & Sons, Chichester, United Kingdom, 5th edition. ch6, p. 238.

[28] Parhi, P. S., Garanayak, L., Mahamaya, M., & Das, S. K. (2017). Stabilization of an Expansive Soil Using Alkali Activated Fly Ash Based Geopolymer. Advances in Characterization and Analysis of Expansive Soils and Rocks, 36–50. doi:10.1007/978-3-319-61931-6_4.

[29] Borges, P. H. R., Nunes, V. A., Panzera, T. H., Schileo, G., & Feteira, A. (2016). The Influence of Rice Husk Ash Addition on the Properties of Metakaolin-Based Geopolymers. The Open Construction & Building Technology Journal, 10(1), 406–417. doi:10.2174/1874836801610010406.

[30] Cheng, F., Li, W., Zhou, Y., Shen, J., Wu, Z., Liu, G., Lee, P. W., & Tang, Y. (2012). AdmetSAR: A comprehensive source and free tool for assessment of chemical ADMET properties. Journal of Chemical Information and Modeling, 52(11), 3099–3105. doi:10.1021/ci300367a.

[31] Xi, Y., Wu, X., & Xiong, H. (2014). Solidification/Stabilization of Pb-contaminated Soils with Cement and Other Additives. Soil and Sediment Contamination: An International Journal, 23(8), 887–898. doi:10.1080/15320383.2014.890168.

[32] Fernández-Jiménez, A., & Palomo, A. (2003). Characterisation of fly ashes. Potential reactivity as alkaline cements. Fuel, 82(18), 2259–2265. doi:10.1016/S0016-2361(03)00194-7.

[33] Moon, D. H., & Dermatas, D. (2006). An evaluation of lead leachability from stabilized/solidified soils under modified semi-dynamic leaching conditions. Engineering Geology, 85(1–2), 67–74. doi:10.1016/j.enggeo.2005.09.028.

[34] Garcia-Lodeiro, I., Palomo, A., Fernández-Jiménez, A., & MacPhee, D. E. (2011). Compatibility studies between N-A-S-H and C-A-S-H gels. Study in the ternary diagram Na2O-CaO-Al2O3-SiO 2-H2O. Cement and Concrete Research, 41(9), 923–931. doi:10.1016/j.cemconres.2011.05.006.

[35] Abdul Hussein Saeed, K., Kassim, K. A., Mohd Yunus, N. Z., & Nur, H. (2015). Physico-Chemical Characterization Of Lime Stabilized Tropical Kaolin Clay. Jurnal Teknologi, 72(3). doi:10.11113/jt.v72.4021.

[36] Steveson, M., & Sagoe-Crentsil, K. (2005). Relationships between composition, structure and strength of inorganic polymers. Journal of Materials Science, 40(8), 2023–2036. doi:10.1007/s10853-005-1226-2.

[37] Li, Q., Chen, J., Shi, Q., & Zhao, S. (2014). Macroscopic and microscopic mechanisms of cement-stabilized soft clay mixed with seawater by adding ultrafine silica fume. Advances in Materials Science and Engineering, 2014, 2014. doi:10.1155/2014/810652.

[38] Sturm, P., Gluth, G. J. G., Brouwers, H. J. H., & Kühne, H. C. (2016). Synthesizing one-part geopolymers from rice husk ash. Construction and Building Materials, 124, 961–966. doi:10.1016/j.conbuildmat.2016.08.017.

[39] Vesic, A. S. (1975). Bearing capacity of shallow foundations. Foundation engineering handbook, Van Nostrand Reinhold, New York, United States.